

Article

Construction of a Dengue NanoLuc Reporter Virus for In Vivo Live Imaging in Mice

Enyue Fang^{1,2,†}, Xiaohui Liu^{1,†}, Miao Li^{1,†}, Jingjing Liu^{1,†}, Zelun Zhang¹, Xinyu Liu¹, Xingxing Li¹, Wenjuan Li¹, Qinhua Peng¹, Yongxin Yu^{1,*} and Yuhua Li^{1,*}

¹ Department of Arbovirus Vaccine, National Institutes for Food and Drug Control, Beijing 102629, China; dlu_fangenyue@163.com (E.F.); liux1aohui@163.com (X.L.); limiao1711@163.com (M.L.); liujingjing@nifdc.org.cn (J.L.); zelun128@hotmail.com (Z.Z.); liuxinyu@nifdc.org.cn (X.L.); lxx0320@outlook.com (X.L.); wenjuan279@outlook.com (W.L.); pengqinhua666@163.com (Q.P.)

² Wuhan Institute of Biological Products, Co., Ltd., Wuhan 430207, China

* Correspondence: yuyongxin@nifdc.org.cn (Y.Y.); liyuhua@nifdc.org.cn (Y.L.); Tel.: +86-010-5385-2137 (Y.Y.); +86-010-5385-2128 (Y.L.)

† These authors contributed equally to this work.

Abstract: Since the first isolation in 1943, the dengue virus (DENV) has spread throughout the world, but effective antiviral drugs or vaccines are still not available. To provide a more stable reporter DENV for vaccine development and antiviral drug screening, we constructed a reporter DENV containing the NanoLuc reporter gene, which was inserted into the 5' untranslated region and capsid junction region, enabling rapid virus rescue by in vitro ligation. In addition, we established a live imaging mouse model and found that the reporter virus maintained the neurovirulence of prototype DENV before engineering. DENV-4 exhibited dramatically increased neurovirulence following a glycosylation site-defective mutation in the envelope protein. Significant mice mortality with neurological onset symptoms was observed after intracranial infection of wild-type (WT) mice, thus providing a visualization tool for DENV virulence assessment. Using this model, DENV was detected in the intestinal tissues of WT mice after infection, suggesting that intestinal lymphoid tissues play an essential role in DENV pathogenesis.

Keywords: flavivirus; reporter virus; in vivo imaging; neurovirulence



Citation: Fang, E.; Liu, X.; Li, M.; Liu, J.; Zhang, Z.; Liu, X.; Li, X.; Li, W.; Peng, Q.; Yu, Y.; et al. Construction of a Dengue NanoLuc Reporter Virus for In Vivo Live Imaging in Mice. *Viruses* **2022**, *14*, 1253. <https://doi.org/10.3390/v14061253>

Academic Editor: Qiang Ding

Received: 25 April 2022

Accepted: 7 June 2022

Published: 9 June 2022

Publisher's Note: MDPI stays neutral with regard to jurisdictional claims in published maps and institutional affiliations.



Copyright: © 2022 by the authors. Licensee MDPI, Basel, Switzerland. This article is an open access article distributed under the terms and conditions of the Creative Commons Attribution (CC BY) license (<https://creativecommons.org/licenses/by/4.0/>).

1. Introduction

It has been nearly 80 years since the first dengue virus (DENV) was isolated in 1943. Four DENV serotypes are now circulating worldwide, with infection in more than 100 countries and nearly 3.6 billion people at risk of infection [1]. With the rise of reverse genetics technology, recombinant virus design has been widely used in basic research on RNA viruses and vaccine development, which has played a key role in the prevention and control of DENV and other flaviviruses [2,3]. In particular, reporter viruses are widely used as a molecular tool for antiviral drug screening [4,5], neutralizing antibody quantification [6–11], vaccine development [12], and pathogenesis research [13,14].

Originally, reporter viruses were constructed by inserting the reporter gene into a permissive site in the 3' untranslated region (UTR) under the control of an internal ribosomal entry site [15–17]. Despite short-term success, these reporter viruses were prone to loss of reporter genes due to recombination, which made them unstable. Subsequently, a different and more stable method of inserting the reporter gene was developed for yellow fever virus. It is important to insert the reporter gene into the linkage region between the 5' UTR and the capsid gene, but because of RNA regulatory elements that are continuous from the 5' UTR to the capsid gene, a portion of the capsid gene must be duplicated upstream of the reporter gene [18]. Further improvements to achieve long-term stability (i.e., stable for ten passages in cell culture) have been developed. Besides using

split reporter systems, codon optimization of the capsid gene to reduce homology and optimization of capsid duplication length can increase reporter stability [19]. Although these new approaches can improve reporter virus construction, the insertion of reporter genes into the viral genome as exogenous genes can reduce the virulence of engineered flaviviruses. Such attenuation weakens the utility of current reporter viruses when studying viral replication and pathogenesis.

Mice are not sensitive to DENV; in the early stage, intracranial infection of wild-type (WT) mice is often used for virulence evaluation by natural survival [20,21]. The DENV Ban18 strain isolated from mosquitoes in Xishuangbanna, Yunnan, China, in 1981 has strong neurovirulence in mice. Subsequently, the Ban18HK20 strain, attenuated for mice, was obtained by successive passages on primary hamster kidney cells for 20 generations [22]. We previously found that amino acid 155 of the E protein of the Ban18 strain is a key site affecting virus virulence. Intracranial infection of BALB/c mice with a glycosylation site-defective mutation at amino acid 155 (T155I) in the envelope (E) protein of DENV-4 Ban18HK20 strain resulted in neurological morbidity and mortality in mice with significantly increased neurovirulence. However, this method does not allow the observation of the virus infection cycle *in vivo*, which is not conducive to the study of pathogenesis. Although a reporter DENV, based on a conventional luciferase construct, could be visualized *in vivo* in mice [13], a stable reporter virus still only allows the insertion of small exogenous genes. The insertion of reporter genes of proteins with large molecular weight into flaviviruses can attenuate the pathogenicity and affect the virulence mechanisms of these viruses in relevant applications [19]. In this study, we used the gene of NanoLuc luciferase, which has a low molecular weight and high luminescence intensity, to construct a reporter DENV. For the study of the pathogenesis and virulence of DENV, we also established a live imaging mouse model to provide a visualization tool for observing the dynamic process of DENV infection for a continuous period without dissecting mice.

2. Materials and Methods

2.1. Viruses, Plasmids, and Cells

The neurovirulent DENV-4 Ban18 strain was isolated in 1981 from Xishuangbanna, Yunnan, China. Following 20 consecutive passages of Ban18 in primary hamster kidney cells, the non-neurovirulent DENV-4 Ban18HK20 strain was obtained. Both strains are preserved in the Division of Arboviral Vaccines, National Institutes for Food and Drug Control (NIFDC), China. Infectious clone plasmids pSPTM-DENV(WT) and pSPTM-DENV(T155I) against the DENV-4 Ban18HK20 strain and its E protein amino acid mutant strain (with mutation at position 155), as well as their rescued viruses, are preserved in the Division of Arboviral Vaccines, NIFDC. Vero cells were derived from ATCC and cultured in DMEM supplemented with 10% fetal bovine serum. Four-week-old BALB/c mice without specific pathogens were supplied by the Center of Animal Breeding, NIFDC.

2.2. Molecular Cloning Strategy

The NanoLuc reporter gene was derived from the commercial plasmid pNL1.1[NLuc] Vector (Cat. N1001; Promega, Madison, WI, USA). To make NanoLuc more stable when inserted into the viral genome as an exogenous gene, it was inserted following the coding sequence of the first 38 amino acids from the 5' end of the DENV capsid gene, connected by a self-cleaving peptide coding sequence of *Thosea asigna* virus 2A (T2A). In addition, the coding sequence of the first 38 amino acids of the codon-optimized capsid gene (C38) was inserted following the T2A sequence to prevent the loss of the NanoLuc reporter gene by homologous recombination of the two C38 sequences.

Because of the presence of the DENV gene, which is toxic to bacteria, in the target sequence, the plasmid of the recombinant reporter virus cannot be stably replicated in *E. coli*. Therefore, the full length of the target sequence was divided into two sequences (A and B) to construct subcloned plasmids, and then the virus was rescued by enzymatic digestion and *in vitro* ligation of the two linear fragments (Figure 1B).

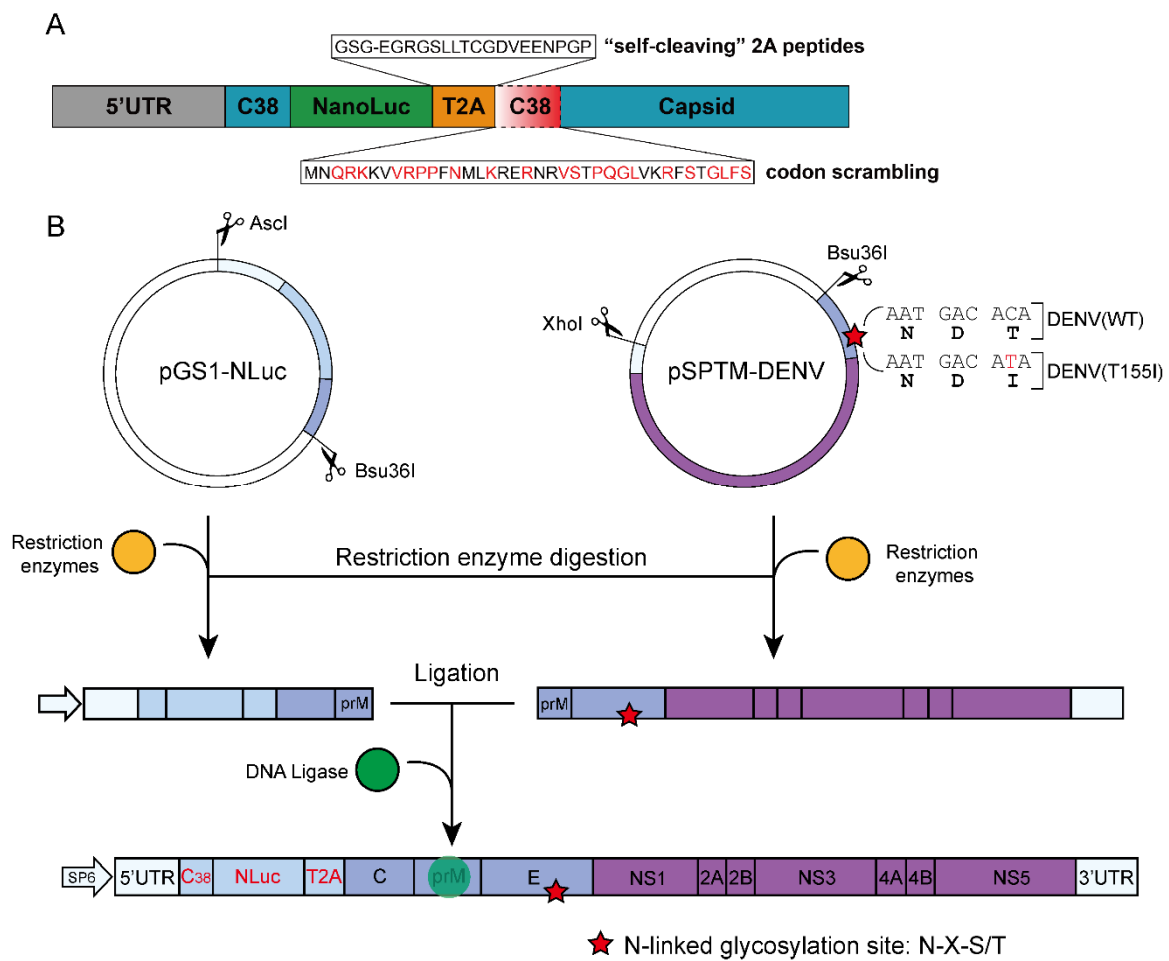


Figure 1. Construction of reporter DENV. (A) Construction design of the NanoLuc reporter gene. NanoLuc was linked to the capsid gene by the T2A sequence and was flanked by duplicate sequences of the capsid gene. (B) In vitro ligation of full-length cDNA of reporter DENV. Two reporter viruses were constructed, one based on WT DENV, and the other based on a glycosylation site-defective mutation in the E protein.

Briefly, first, the NanoLuc+T2A+C38_{codon scrambling} gene (690 bp) was synthesized. The subcloned plasmid pGS1-NLuc containing the genes of pSPTM-DENV(WT)-Ascl-terminal sequence (1–241 bp), NanoLuc+T2A+C38_{codon scrambling} sequence (690 bp), and pSPTM-DENV(WT)-Bsu36l-terminal sequence (242–657 bp) was constructed using the In-Fusion Cloning Kit (Cat. 639650; TaKaRa Bio Inc., Kusatsu, Shiga, Japan). The plasmid was digested with Ascl and Bsu36l, followed by treatment with calf intestinal alkaline phosphatase (CIAP), and the target sequence A (1336 bp) was obtained by electrophoresis and gel recovery. Subsequently, the pSPTM-DENV(WT) infectious clone plasmid was digested with XhoI, the sticky ends were digested with mung bean nuclease, and the linearized DNA was purified after treatment with CIAP. The recovered DNA was then digested with Bsu36l, and the target sequence B (10,043 bp) was obtained by electrophoresis, followed by gel cutting and recovery. Finally, sequences A and B were ligated at a molar concentration ratio of 3:1 in the presence of T4 ligase to obtain a full-length cDNA sequence. After electrophoresis, the ligated products were excised from the gel and used as transcriptional templates for subsequent experiments.

2.3. In Vitro Transcription and Virus Rescue

Full-length linear DNA obtained by in vitro ligation was used as a template for in vitro transcription using SP6 Transcription Reagent (Cat. P1280; Promega) and m7G Cap Analog

(Cat. P1712; Promega). RNA was purified using the RNeasy MinElute Cleanup Kit (Cat. 74204; Qiagen, Valencia, CA, USA), and the recovered RNA was electrotransfected into Vero cells by the Gene Pulser Xcell electroporation system (Bio-Rad, Hercules, CA, USA) using the following settings: voltage: 220 V, capacitor: 300 μ F, cuvette gap: 0.4 cm, resistor: none. Obvious cytopathic effects were observed after 5–7 days of cell culture, and the cell supernatant was collected as the rescued virus, centrifuged, and aliquoted for freezing at -80 °C.

2.4. Virus Titer Assay

Vero cells were grown in a six-well plate with 1×10^6 cells/well. When the confluence reached 80–90%, the supernatant was discarded, and the virus at 10-fold serial dilution (10^{-1} – 10^{-6}) was added to the six-well plate and incubated at 37 °C for 1 h. Excess virus was discarded, methylcellulose was added, and incubation was continued for 7 days. Plaques were counted after crystal violet staining. One plaque was considered one plaque forming unit (PFU), and the virus titer was defined as lg (PFU/mL).

2.5. NLuc Expression in Vero Cells

Vero cells were infected with DENV(WT)-NLuc and DENV(T155I)-NLuc at multiplicity of infection (MOI) of 0.1, and a blank control was established with cells not infected with the virus. Intracellular fluorescence expression was detected at 5 DAI when significant cytopathic effects could be observed. The substrate was diluted 1:50 with phosphate-buffered saline (PBS) in Nano-Glo[®] Luciferase Assay (Cat. N1110; Promega), mixed with cells in equal volume, and placed in the GloMax 96 microplate luminometer (Promega) for detection.

2.6. RT-PCR and Viral Genome Sequencing

Viral RNA was extracted and reverse transcribed into cDNA. Primers were designed for the 5' and 3' ends of the NLuc gene for RT-PCR, and the amplified products were electrophoresed to observe whether the band sizes were correct. Primers were also designed for the complete reporter DENV gene sequence. The whole length of the viral genome was amplified by segmentation, and the amplification products were sequenced.

2.7. Virus Plaque Purification Assay

The virus to be purified was inoculated into Vero cells after 10-fold serial dilution (10^{-1} – 10^{-6}) and adsorbed at 37 °C for 1 h. The virus in the plate was discarded, and the first layer of agar overlay was added and incubated at 37 °C for 5 days. Subsequently, a second layer of agar overlay containing neutral red staining solution was added, and incubation was continued for 24 h. The monoclonal virus strain was selected under light and cultured in a six-well plate containing Vero cells.

2.8. In Vivo Imaging and Dynamics in Mice

Neurovirulence and neuroinvasiveness of the recombinant reporter virus were detected in 4-week-old (13–15 g) BALB/c mice. The neurovirulence group was injected intracerebrally with 0.03 mL of virus (4.4 lg PFU). The neuroinvasiveness group was injected subcutaneously with 0.1 mL of virus (5.0 lg PFU) and intracerebrally (right side) with PBS. Prototype DENV without the reporter gene was used as a control. Fluorescence was detected in the same mice from each group at 0 (12 h), 3, 5, 7, and 9 DAI. The heart, liver, spleen, lung, kidney, brain, and intestinal tissues of mice were dissected at 7 DAI, and the fluorescence intensity was measured. For in vivo imaging of mice, the Nano-Glo substrate was diluted 1:40 with PBS and injected into the orbit. After 10 min of administration, mice or tissue organs were placed in the IVIS[®] Spectrum in vivo imaging system (Perkin-Elmer, Waltham, MA, USA) to detect luminescence intensity. In addition, five mice in each group were infected in the same manner, and their body weight changes and survival were monitored daily.

2.9. Statistical Analysis

Statistical analysis was performed using GraphPad Prism 9 (GraphPad Software Inc., San Diego, CA, USA). One-way analysis of variance (ANOVA) was used to determine statistical differences between groups in luciferase activity of Vero cells after reporter DENV infection, and Tukey's method was used for multiple comparisons. Statistical significance of the fluorescence signals in mice infected with the reporter virus was determined using two-way ANOVA. $p < 0.05$ was considered significant for differences between sample groups.

3. Results

3.1. Construction and Biological Properties of Reporter DENV

To construct a more stable reporter DENV, the NanoLuc reporter gene was engineered at the capsid gene region, and the capsid gene sequence was duplicated to flank the reporter gene (Figure 1A). Such duplication of the coding sequence of the 38 amino acids in the capsid gene (C38) is essential for viral replication, and the beginning of the capsid gene was codon scrambled to minimize homology with the duplicated portion [23]. The reporter gene was linked to the capsid gene by the T2A self-cleaving peptide sequence, and a glycine-serine-glycine (GSG) linker was added to the N-terminus of the 2A peptide sequence to improve the efficiency of the 2A peptide-induced cleavage [24]. Because DENV genes are toxic to bacteria, rapidly constructing a stable full-length cDNA infectious clone is difficult. Therefore, a full-length cDNA template for transcription was constructed by ligation of two linear fragments *in vitro*, and the recombinant virus was rescued by electrotransfection. Thus, two types of recombinant reporter DENVs were constructed: (i) DENV(WT)-NLuc, based on the WT DENV-4 Ban18HK20 strain; and (ii) DENV(T155I)-NLuc, based on the mutant DENV-4 Ban18HK20 strain with the glycosylation site-defective mutation (Figure 1B).

The full-length cDNA sequence of the reporter virus was obtained *in vitro* by ligation with T4 DNA ligase. The electrophoresis results of the purified ligated product are shown in Figure 2A, with molecular weight above 10 kb and correct band size, which was used as a template for *in vitro* transcription in subsequent virus rescue. The two strains of reporter DENV were titrated at 6.23 lg PFU/mL for DENV(WT)-NLuc and 6.30 lg PFU/mL for DENV(T155I)-NLuc, and both showed similar plaque size (Figure 2B). Significantly higher fluorescence activity was detected after infection of Vero cells by both reporter viruses compared with the blank control (Figure 2C).

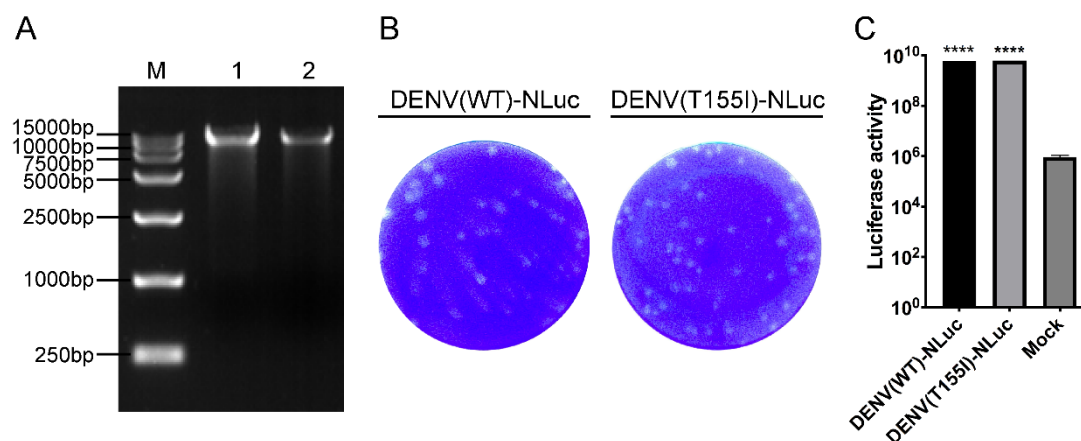


Figure 2. Construction and biological properties of DENV(WT)-NLuc and DENV(T155I)-NLuc. (A) DENV-NLuc full-length linear sequence ligated *in vitro* with T4 DNA ligase. M: DL15000 marker; 1: DENV(WT)-NLuc linkage products; 2: DENV(T155I)-NLuc linkage products. (B) Plaque morphology of DENV with the NanoLuc reporter gene. The dilution factor was 10^{-4} -fold. (C) Luciferase activity of Vero cells after infection of reporter DENV. ****, $p \leq 0.0001$ compared with Vero cells in the mock group.

3.2. Plaque Purification and Sequencing of Reporter DENV

Using prototype DENV without the NanoLuc reporter gene as a control, RNA from the reporter and control viruses was extracted, and primers were designed upstream and downstream of the reporter gene region for reverse transcription-polymerase chain reaction (RT-PCR) amplification. The amplified bands of the two recombinant reporter DENVs were of the correct size but abnormal (Figure 3A), suggesting that the recombinant viruses obtained using this method were impure and required to be purified by plaque selection. Therefore, five purified monoclonal strains of each of the two reporter viruses were isolated and cultured. RT-PCR results showed that DENV(WT)-NLuc clones 2–5 and DENV(T155I)-NLuc clones 1–5 were amplified with bands of the correct size (Figure 3B). Viral genome sequencing results showed that the purified monoclonal strains 1, 2, 3, and 4 of DENV(WT)-NLuc contained nucleotide mutations (Table 1), whereas the other purified strains contained non-nucleotide mutations and could be used for subsequent study.

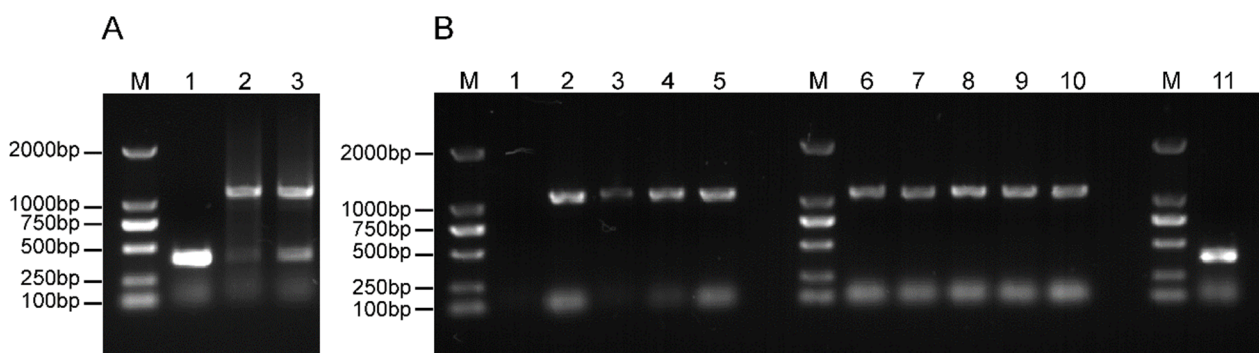


Figure 3. RT-PCR electrophoresis of reporter DENV. (A) RT-PCR of impure reporter DENV. Primers were designed to start at the 5' UTR and end at the capsid gene, and the amplified fragment size was 1094 bp. The inserted NLuc fragment size was 690 bp. M: DL2000 marker; 1: DENV(WT); 2: DENV(WT)-NLuc; 3: DENV(T155I)-NLuc. (B) RT-PCR of plaque-purified reporter DENV. The amplified fragment of the virus with the NanoLuc reporter gene was 1094 bp, and the amplified fragment of the virus without the NanoLuc reporter gene was 690 bp. M: DL2000 marker; 1: DENV(WT)-NLuc-puri1; 2: DENV(WT)-NLuc-puri2; 3: DENV(WT)-NLuc-puri3; 4: DENV(WT)-NLuc-puri4; 5: DENV(WT)-NLuc-puri5; 6: DENV(T155I)-NLuc-puri1; 7: DENV(T155I)-NLuc-puri2; 8: DENV(T155I)-NLuc-puri3; 9: DENV(T155I)-NLuc-puri4; 10: DENV(T155I)-NLuc-puri5; 11: DENV(WT).

Table 1. Sequencing of plaque-purified strains of DENV with the NanoLuc reporter gene.

Sample	Mutation											
	NLuc-82	NLuc-118	T2A-14	C-1	C-15	E-224	E-241	NS1-213	NS3-14	NS3-230	NS4B-5	NS5-689
DENV(WT)-NLuc	GTG(V)	GGC(G)	GAA(E)	ATG(M)	CTG(L)	GCA(A)	AAG(K)	GAG(E)	CAG(Q)	GAG(E)	CTG(L)	AGG(R)
DENV(WT)-NLuc-puri1	-	aGC(S)	-	-	-	GCt(A)	-	-	-	-	-	-
DENV(WT)-NLuc-puri2	cTG(L)	-	-	-	CtA(L)	-	AAa(K)	-	-	GAA(E)	CtA(L)	AGa(R)
DENV(WT)-NLuc-puri3	-	-	aAA(K)	-	-	-	-	GAa(E)	CAa(Q)	-	-	-
DENV(WT)-NLuc-puri4	-	-	-	ATa(I)	-	-	-	-	-	-	-	-
DENV(WT)-NLuc-puri5	-	-	-	-	-	-	-	-	-	-	-	-
DENV(T155I)-NLuc-puri1	-	-	-	-	-	-	-	-	-	-	-	-
DENV(T155I)-NLuc-puri2	-	-	-	-	-	-	-	-	-	-	-	-
DENV(T155I)-NLuc-puri3	-	-	-	-	-	-	-	-	-	-	-	-
DENV(T155I)-NLuc-puri4	-	-	-	-	-	-	-	-	-	-	-	-
DENV(T155I)-NLuc-puri5	-	-	-	-	-	-	-	-	-	-	-	-

3.3. Characterization of In Vivo Propagation of Reporter DENV

DENV(WT)-NLuc and DENV(T155I)-NLuc intracerebrally injected mice were imaged in vivo on different days after infection (DAI). DENV(WT)-NLuc fluorescence was undetectable at 7 DAI, and slight fluorescence was detected in the brain at 9 DAI, whereas DENV(T155I)-NLuc was detected in the brain at 3 DAI, and the fluorescence intensity in the brain continued to increase (Figure 4). In addition, fluorescence of DENV(T155I)-NLuc was detected in the mouse peritoneal cavity at 7 DAI (Figure 4), and dissection of organs for

fluorescence imaging showed that fluorescence was detectable in mouse intestinal tissues (Figure 5). Subsequently, the reporter virus in mouse intestinal tissues was transient in repeated trials.

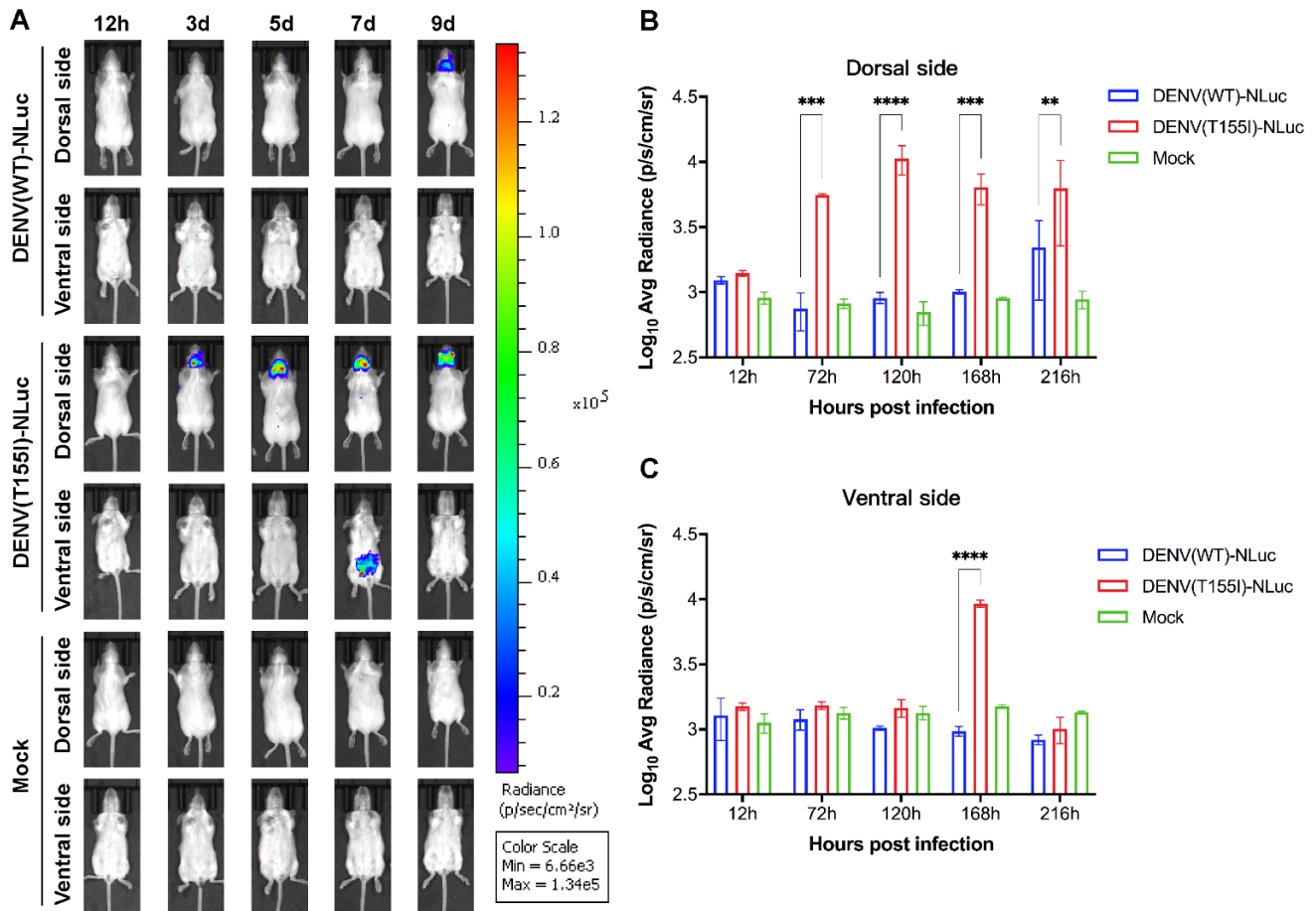


Figure 4. In vivo imaging of reporter DENV intracerebral infection of 4-week-old BALB/c mice. (A) BALB/c mice ($n = 3$) were injected intracerebrally with 4.4 lg PFU of the reporter virus, and fluorescence signals of the dorsal and ventral sides of mice at different time points. A representative animal from each group is shown. (B) Average luminescence intensity of the dorsal side of mice at different time points. (C) Average luminescence intensity of the ventral side of mice at different time points. Data are derived from two independent experiments. Statistical significance was determined using two-way ANOVA. **, ***, and **** indicate $p \leq 0.01$, 0.001, and 0.0001, respectively, compared with the fluorescence signals in the DENV(WT)-NLuc group.

3.4. Similar Neurovirulence in Reporter and Prototype DENVs

Generally, the insertion of exogenous genes into the viral genome can reduce virus virulence. To determine whether the virulence of the constructed reporter DENV is altered in mice, we injected mice with the recombinant reporter virus and prototype virus (without the reporter gene) by two routes of infection—intracerebral and subcutaneous, followed by intracerebral blank injection. The results of the intracerebral infection group showed that DENV(T155I)-NLuc had reduced neurovirulence, and the mortality rate of mice was reduced from 100% to 80% compared with DENV(T155I) that was not inserted with the NanoLuc reporter gene, but both groups had a significant reduction in body weight (Figures 6 and 7). The results of the subcutaneous infection group showed that neither the reporter virus nor the prototype virus was neuroinvasive in mice, and no fluorescence was detected. The recombinant reporter virus had properties similar to the prototype virus, and the insertion of the reporter gene could retain the high DENV neurovirulence and the same

symptoms of mice pathogenesis as the prototype virus, indicating that this model could be used for studies related to DENV virulence mechanism and antiviral drug screening.

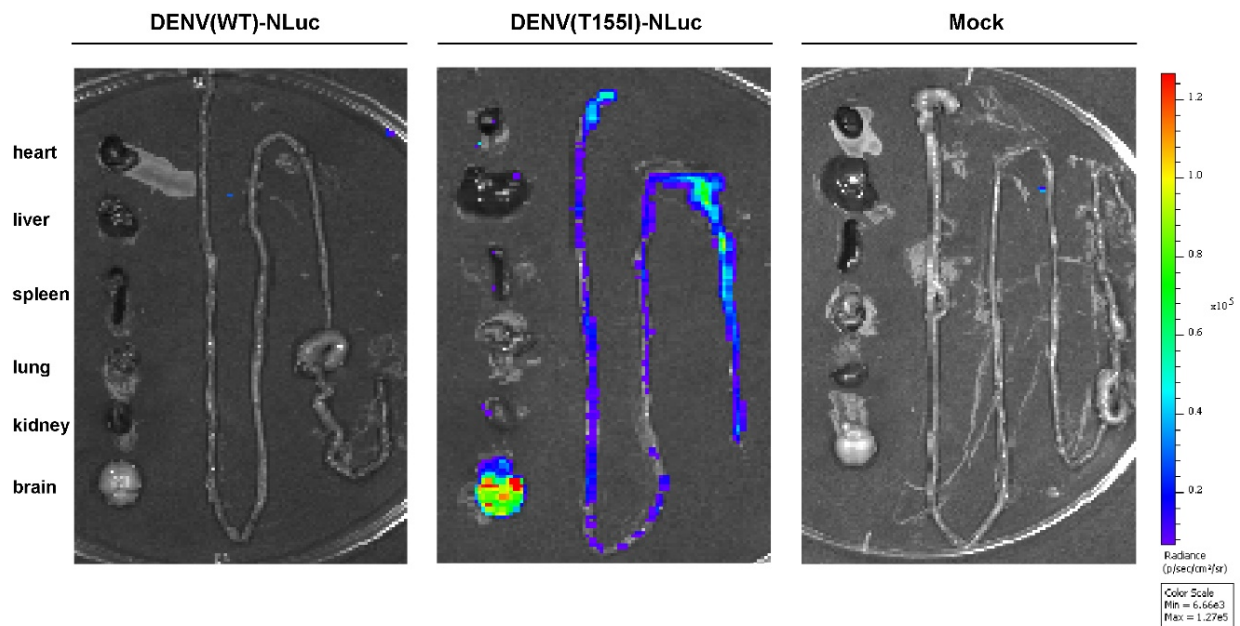


Figure 5. Fluorescence of tissues from major organs of mice on day 7 after intracerebral infection. BALB/c mice ($n = 3$) were injected intracerebrally with a dose of 4.4 lg PFU of virus, and heart, liver, spleen, lung, kidney, brain, and intestinal tissues were dissected for fluorescence detection at 7 DAI. Independent experiments were performed twice. Representative animal tissues from organs of each group are shown.

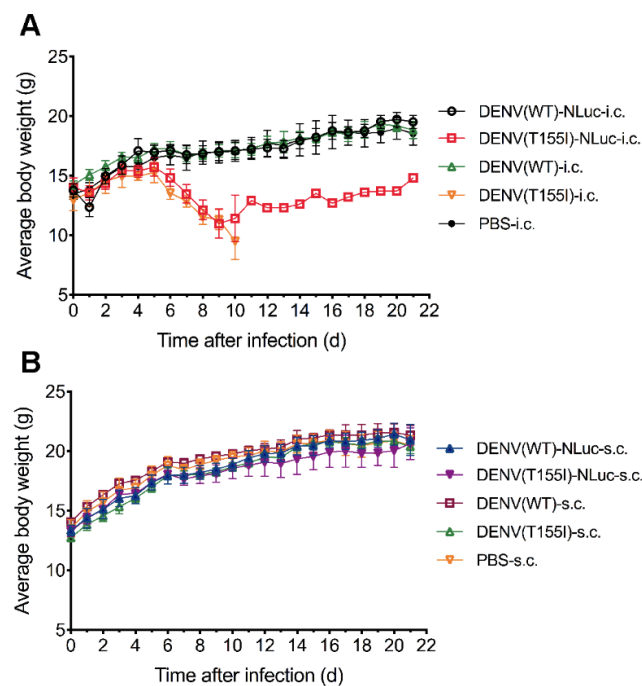


Figure 6. Body weight monitoring of 4-week-old BALB/c mice injected with prototype and reporter DENVs. (A) BALB/c mice ($n = 5$) were injected intracerebrally with 0.03 mL of virus (4.4 lg PFU). (B) BALB/c mice ($n = 5$) were injected subcutaneously with 0.1 mL of virus (5.0 lg PFU) and intracerebrally (right side) with PBS. Body weight of mice was monitored daily.

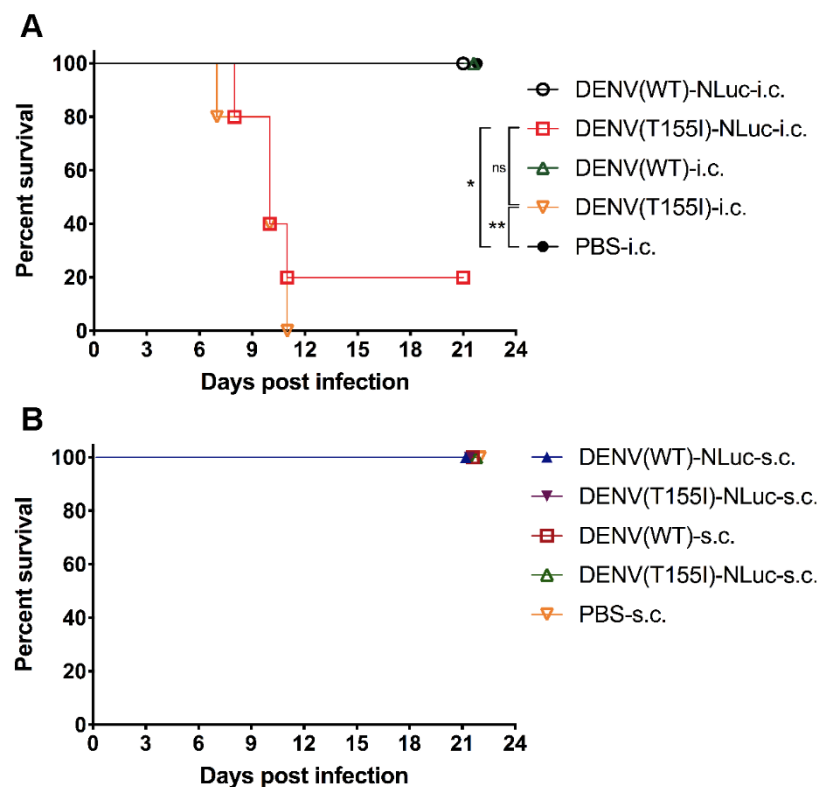


Figure 7. Survival curve of 4-week-old BALB/c mice injected with prototype and reporter DENVs. (A) BALB/c mice ($n = 5$) were injected intracerebrally with 0.03 mL of virus (4.4 lg PFU). (B) BALB/c mice ($n = 5$) were injected subcutaneously with 0.1 mL of virus (5.0 lg PFU) and intracerebrally (right side) with PBS. Animals were observed for 3 weeks after challenge and were euthanized when humane endpoints were reached. Log-rank (Mantel–Cox) survival analysis test was performed to determine statistical significance. *, $p \leq 0.05$; **, $p \leq 0.01$; ns, no statistical significance.

4. Discussion

Ever since the first reporter flavivirus was reported in 2003 [15], many types of reporter viruses have been widely used in high-throughput antiviral drug screening [4], host–virus pathogenesis studies [25], and serological diagnosis [9]. Despite their several advantages, reporter flaviviruses still face the challenges of genetic instability and susceptibility to recombination-mediated loss of reporter genes during virus passaging [16].

To analyze the pathogenic mechanism of highly neurovirulent mutant strains of DENV and the infection of attenuated strains in mice, we constructed reporter viruses to perform live imaging in mice to observe the tropism and dynamic distribution of DENV infection. However, because the conventional fluorescent reporter gene is large, its insertion into the viral genome adversely affects the genetic stability and virulence of the virus, making its application difficult in animal model studies of virulence. Therefore, NanoLuc, a luciferase recently developed by Promega, was used in this study. With a low molecular weight (19.1 kDa, 171 amino acids), NanoLuc can be used for enhanced viral delivery and protein fusion, is easily secreted by cells, and is widely used in reporter flavivirus construction [7,23,26–29]. Moreover, the NanoLuc system displayed a specific activity over 150-fold higher than both North American Firefly (FLuc) and Renilla (RLuc) luciferases, providing better performance in cells that are difficult to transfect [30,31]. Although NanoLuc luciferase has a low molecular weight, it may still encounter problems with replication stability and expression or secretion as a heterologous protein when its gene is inserted directly into the DENV genome. To avoid these problems, the reporter gene was inserted between the 5' UTR and the capsid gene. The initial amino acid-coding sequence of the capsid gene (C38) was added to the 5' end of the reporter gene, and the T2A peptide self-cleavage sequence was added to the 3' end of the reporter gene to enable expression

and secretion of the reporter gene. Baker et al. [7,23] used a similar strategy to construct various reporter flaviviruses.

Currently, the four main 2A peptides commonly used for genetic engineering are T2A (Thosea asigna virus 2A), P2A (porcine teschovirus-1 2A), E2A (equine rhinitis A virus), and F2A (foot-and-mouth disease virus) [32,33]. Among these, T2A, P2A, and E2A can achieve almost complete self-cleaving efficiency without detection of polyprotein products, while F2A can achieve a self-cleaving efficiency of more than 90% [24,34–36]. In this study, the T2A peptide self-cleavage sequence was used, and the GSG sequence was added to the N-terminus of the 2A peptide sequence to improve the 2A peptide-induced cleavage efficiency [24]. Finally, to prevent homologous recombination between the C38 sequence added to the 5' end of the reporter gene and the capsid gene sequence following T2A, the coding sequence of the first 38 amino acids of the capsid gene was codon optimized, thereby disrupting its nucleotide sequence to avoid homologous recombination and improving the stability of the recombinant reporter virus.

Based on this construction strategy, we initially attempted to construct an infectious clone plasmid by inserting the NanoLuc reporter gene directly into the DENV genome. However, because of the presence of toxicity genes in the flavivirus genome, it is difficult to directly construct infectious clone plasmids containing full-length viral sequences for stable replication in *Escherichia coli* [37,38]. Stable infectious clone plasmids with full-length viral sequences can be obtained by screening different cloning vectors and competent cells, and optimizing culture temperature, incubation time, antibiotic concentration, and shaking speed [39–41]. However, because this approach is time-consuming and laborious, the full length of the viral genome can be divided into multiple sequences for the subclonal construction of flavivirus infectious clone plasmids that are difficult to construct. The enzymatic cleavage sites (e.g., BsmBI and BglII) with opposite orientations (preventing self-ligation) were added to the beginning and end of the target gene of each subclone, followed by in vitro ligation of the linear fragments from multiple subcloned plasmids into the full length of viral cDNA using DNA ligase, which serves as a template for in vitro transcription in virus rescue. Deng et al. [42] rescued Zika virus by such in vitro ligation. Messer et al. [43] also successfully constructed DENV-3 and its chimeric virus using this method. Xie et al. [44,45] also used this method to rapidly construct recombinant severe acute respiratory syndrome coronavirus 2 (SARS-CoV-2) and its reporter virus, which has a larger genome than flavivirus. In this study, we also used the in vitro ligation method for virus rescue and successfully obtained reporter DENV. However, the virus rescued by in vitro ligation is usually of poor purity, and plaque purification is required for screening to obtain a correctly sequenced and genetically stable virus strain.

In this study, two reporter DENVs were constructed: (i) DENV(WT)-NLuc, a reporter virus based on the WT DENV-4 Ban18HK20 strain, which was not neurovirulent in mice; and (ii) DENV(T155I)-NLuc, a reporter virus based on the E protein N-glycosylation site-defective mutation in the mutant strain (T155I) of DENV-4 Ban18HK20, which was highly neurovirulent in mice. We previously found that the virulence of the point mutant virus DENV (T155I) was significantly enhanced after mutating the glycosylation site at amino acid 155 of the E protein of the non-neurovirulent DENV-4 Ban18HK20 strain. The same virulence locus was found in the DENV-4 H241 international standard strain by Kawano et al. [46]. Both virulent and attenuated strains containing the reporter gene were used in the subsequent in vivo live imaging study in mice. The luciferase signal was detected in the brain of DENV(T155I)-NLuc-treated mice at 3 DAI, and the expression increased day by day. The mice showed significant neurological symptoms at 7 DAI, and luciferase signals that were observed in the peritoneal cavity of mice were also detected in the intestinal tissues after dissection. Schoggins et al. [13] also detected a strong luciferase signal in gut-associated lymphoid tissue after infection of interferon receptor-deficient mice using reporter DENV. Zellweger et al. [47] detected viral RNA in the small intestine of AG129 mice after DENV-2 infection. They performed antibody-dependent enhancement experiments in which a high viral load was detected in mice in the presence of subneutraliz-

ing levels of DENV-specific antibodies. Moreover, significant gastrointestinal bleeding was observed in mice 84 h after infection, which is an important clinical hallmark of dengue hemorrhagic fever and dengue shock syndrome in humans [48]. In this study, DENV could be detected in the intestinal tissues of WT mice after infection. However, no luciferase signal was observed in the mouse intestinal tissues at 9 DAI, and subsequent retests showed that the luciferase signal in the mouse intestinal tissues was transient. Thus, intestinal lymphoid tissues may play an essential role in DENV pathogenesis. In addition, a slight luciferase signal was observed in the brain of DENV(WT)-NLuc-treated mice with no signs of morbidity at 9 DAI. Thus, the recombinant reporter virus had similar properties and virulence to prototype DENV without the reporter gene, indicating that the live imaging mouse model can be used for studies related to the virulence mechanism and antiviral drug screening of DENV.

5. Conclusions

NanoLuc luciferase has the twin advantages of high luminescence intensity and low molecular weight. In this study, the NanoLuc reporter gene was successfully inserted into the DENV genome to construct reporter DENVs DENV(WT)-NLuc and DENV(T155I)-NLuc based on the attenuated and virulent strains, respectively. Moreover, an *in vivo* imaging mouse model of intracerebral infection, which maintained DENV neurovirulence in mice, was established, thereby providing a visualization tool for the pathogenesis and antiviral drug screening of DENV. Using this model, DENV could be detected in the intestinal tissues of WT mice after infection, indicating that intestinal lymphoid tissues may play an important role in DENV pathogenesis.

Author Contributions: E.F., J.L., Y.L. and Y.Y. conceived and designed the study. E.F., X.L. (Xiaohui Liu), M.L., Z.Z., X.L. (Xingxing Li), W.L. and Q.P. performed the experiments. X.L. (Xinyu Liu) provided technical support. E.F. analyzed the data and wrote the manuscript. All authors have read and agreed to the published version of the manuscript.

Funding: This research received no external funding.

Institutional Review Board Statement: All animal studies were approved by the Experimental Animal Welfare and Ethics Committee of the National Institutes for Food and Drug Control, China (approval code: 2019(A) 062), and were conducted according to institutional guidelines.

Informed Consent Statement: Not applicable.

Data Availability Statement: All data are available from the corresponding authors upon request.

Conflicts of Interest: The authors declare that there are no conflict of interest regarding the publication of this article.

References

1. Diamond, M.S.; Pierson, T.C. Molecular Insight into Dengue Virus Pathogenesis and Its Implications for Disease Control. *Cell* **2015**, *162*, 488–492. [[CrossRef](#)]
2. Aubry, F.; Nougairède, A.; Gould, E.A.; de Lamballerie, X. Flavivirus reverse genetic systems, construction techniques and applications: A historical perspective. *Antiviral Res.* **2015**, *114*, 67–85. [[CrossRef](#)] [[PubMed](#)]
3. Fang, E.; Liu, X.; Liu, X.; Li, M.; Wang, L.; Li, M.; Zhang, Z.; Li, Y.; Yu, Y. Investigation of immune response induction by Japanese encephalitis live-attenuated and chimeric vaccines in mice. *MedComm* **2022**, *3*, e117. [[CrossRef](#)] [[PubMed](#)]
4. Zou, G.; Xu, H.Y.; Qing, M.; Wang, Q.Y.; Shi, P.Y. Development and characterization of a stable luciferase dengue virus for high-throughput screening. *Antiviral Res.* **2011**, *91*, 11–19. [[CrossRef](#)] [[PubMed](#)]
5. Xie, X.; Zou, J.; Shan, C.; Yang, Y.; Kum, D.B.; Dallmeier, K.; Neyts, J.; Shi, P.Y. Zika Virus Replicons for Drug Discovery. *EBioMedicine* **2016**, *12*, 156–160. [[CrossRef](#)]
6. Zhang, P.T.; Shan, C.; Li, X.D.; Liu, S.Q.; Deng, C.L.; Ye, H.Q.; Shang, B.D.; Shi, P.Y.; Lv, M.; Shen, B.F.; et al. Generation of a recombinant West Nile virus stably expressing the Gaussia luciferase for neutralization assay. *Virus Res.* **2016**, *211*, 17–24. [[CrossRef](#)]
7. Baker, C.; Xie, X.; Zou, J.; Muruato, A.; Fink, K.; Shi, P.Y. Using recombination-dependent lethal mutations to stabilize reporter flaviviruses for rapid serodiagnosis and drug discovery. *EBioMedicine* **2020**, *57*, 102838. [[CrossRef](#)]

8. Pierson, T.C.; Sánchez, M.D.; Puffer, B.A.; Ahmed, A.A.; Geiss, B.J.; Valentine, L.E.; Altamura, L.A.; Diamond, M.S.; Doms, R.W. A rapid and quantitative assay for measuring antibody-mediated neutralization of West Nile virus infection. *Virology* **2006**, *346*, 53–65. [[CrossRef](#)]
9. Shan, C.; Xie, X.; Ren, P.; Loeffelholz, M.J.; Yang, Y.; Furuya, A.; Dupuis, A.P., II; Kramer, L.D.; Wong, S.J.; Shi, P.Y. A Rapid Zika Diagnostic Assay to Measure Neutralizing Antibodies in Patients. *EBioMedicine* **2017**, *17*, 157–162. [[CrossRef](#)]
10. Frumence, E.; Viranaicken, W.; Gadea, G.; Desprès, P. A GFP Reporter MR766-Based Flow Cytometry Neutralization Test for Rapid Detection of Zika Virus-Neutralizing Antibodies in Serum Specimens. *Vaccines* **2019**, *7*, 66. [[CrossRef](#)]
11. Matsuda, M.; Yamanaka, A.; Yato, K.; Yoshii, K.; Watashi, K.; Aizaki, H.; Konishi, E.; Takasaki, T.; Kato, T.; Muramatsu, M.; et al. High-throughput neutralization assay for multiple flaviviruses based on single-round infectious particles using dengue virus type 1 reporter replicon. *Sci. Rep.* **2018**, *8*, 16624. [[CrossRef](#)]
12. Zhu, R.; Liu, Q.; Huang, W.; Yu, Y.; Wang, Y. Comparison of the replication characteristics of vaccinia virus strains Guang 9 and Tian Tan in vivo and in vitro. *Arch. Virol.* **2014**, *159*, 2587–2596. [[CrossRef](#)]
13. Schoggins, J.W.; Dorner, M.; Feulner, M.; Imanaka, N.; Murphy, M.Y.; Ploss, A.; Rice, C.M. Dengue reporter viruses reveal viral dynamics in interferon receptor-deficient mice and sensitivity to interferon effectors in vitro. *Proc. Natl. Acad. Sci. USA* **2012**, *109*, 14610–14615. [[CrossRef](#)]
14. Shan, C.; Xie, X.; Muruato, A.E.; Rossi, S.L.; Roundy, C.M.; Azar, S.R.; Yang, Y.; Tesh, R.B.; Bourne, N.; Barrett, A.D.; et al. An Infectious cDNA Clone of Zika Virus to Study Viral Virulence, Mosquito Transmission, and Antiviral Inhibitors. *Cell Host Microbe* **2016**, *19*, 891–900. [[CrossRef](#)]
15. Yun, S.I.; Kim, S.Y.; Rice, C.M.; Lee, Y.M. Development and application of a reverse genetics system for Japanese encephalitis virus. *J. Virol.* **2003**, *77*, 6450–6465. [[CrossRef](#)]
16. Pierson, T.C.; Diamond, M.S.; Ahmed, A.A.; Valentine, L.E.; Davis, C.W.; Samuel, M.A.; Hanna, S.L.; Puffer, B.A.; Doms, R.W. An infectious West Nile virus that expresses a GFP reporter gene. *Virology* **2005**, *334*, 28–40. [[CrossRef](#)]
17. Deas, T.S.; Binduga-Gajewska, I.; Tilgner, M.; Ren, P.; Stein, D.A.; Moulton, H.M.; Iversen, P.L.; Kauffman, E.B.; Kramer, L.D.; Shi, P.Y. Inhibition of flavivirus infections by antisense oligomers specifically suppressing viral translation and RNA replication. *J. Virol.* **2005**, *79*, 4599–4609. [[CrossRef](#)]
18. Shustov, A.V.; Mason, P.W.; Frolov, I. Production of pseudoinfectious yellow fever virus with a two-component genome. *J. Virol.* **2007**, *81*, 11737–11748. [[CrossRef](#)]
19. Baker, C.; Shi, P.Y. Construction of Stable Reporter Flaviviruses and Their Applications. *Viruses* **2020**, *12*, 1082. [[CrossRef](#)]
20. Ferreira, G.P.; Figueiredo, L.B.; Coelho, L.F.; Policarpo, A.S., Jr.; Cecilio, A.B.; Ferreira, P.C.; Bonjardim, C.A.; Arantes, R.M.; Campos, M.A.; Kroon, E.G. Dengue virus 3 clinical isolates show different patterns of virulence in experimental mice infection. *Microbes Infect.* **2010**, *12*, 546–554. [[CrossRef](#)]
21. Oliveira, E.R.; Amorim, J.F.; Paes, M.V.; Azevedo, A.S.; Gonçalves, A.J.; Costa, S.M.; Mantuano-Barradas, M.; Póvoa, T.F.; de Meis, J.; Basílio-de-Oliveira, C.A.; et al. Peripheral effects induced in BALB/c mice infected with DENV by the intracerebral route. *Virology* **2016**, *489*, 95–107. [[CrossRef](#)]
22. Fang, E.; Wang, L.; Zhao, D.; Li, M.; Liu, M.; Li, Y. Construction, characterization and stability analysis of infectious clone of live attenuated dengue virus type 4 Ban18HK20 strain. *Chin. J. Microbiol. Immunol.* **2019**, *39*, 827–834.
23. Baker, C.; Liu, Y.; Zou, J.; Muruato, A.; Xie, X.; Shi, P.Y. Identifying optimal capsid duplication length for the stability of reporter flaviviruses. *Emerg. Microbes Infect.* **2020**, *9*, 2256–2265. [[CrossRef](#)]
24. Kim, J.H.; Lee, S.R.; Li, L.H.; Park, H.J.; Park, J.H.; Lee, K.Y.; Kim, M.K.; Shin, B.A.; Choi, S.Y. High cleavage efficiency of a 2A peptide derived from porcine teschovirus-1 in human cell lines, zebrafish and mice. *PLoS ONE* **2011**, *6*, e18556. [[CrossRef](#)]
25. Schoggins, J.W.; Wilson, S.J.; Panis, M.; Murphy, M.Y.; Jones, C.T.; Bieniasz, P.; Rice, C.M. A diverse range of gene products are effectors of the type I interferon antiviral response. *Nature* **2011**, *472*, 481–485. [[CrossRef](#)]
26. Mutso, M.; Saul, S.; Rausalu, K.; Susova, O.; Žusinaite, E.; Mahalingam, S.; Merits, A. Reverse genetic system, genetically stable reporter viruses and packaged subgenomic replicon based on a Brazilian Zika virus isolate. *J. Gen. Virol.* **2017**, *98*, 2712–2724. [[CrossRef](#)]
27. He, Y.; Liu, P.; Wang, T.; Wu, Y.; Lin, X.; Wang, M.; Jia, R.; Zhu, D.; Liu, M.; Zhao, X.; et al. Genetically stable reporter virus, subgenomic replicon and packaging system of duck Tembusu virus based on a reverse genetics system. *Virology* **2019**, *533*, 86–92. [[CrossRef](#)] [[PubMed](#)]
28. Yun, S.I.; Song, B.H.; Woolley, M.E.; Frank, J.C.; Julander, J.G.; Lee, Y.M. Development, Characterization, and Application of Two Reporter-Expressing Recombinant Zika Viruses. *Viruses* **2020**, *12*, 572. [[CrossRef](#)] [[PubMed](#)]
29. Volkova, E.; Tsetsarkin, K.A.; Sippert, E.; Assis, F.; Liu, G.; Rios, M.; Pletnev, A.G. Novel Approach for Insertion of Heterologous Sequences into Full-Length ZIKV Genome Results in Superior Level of Gene Expression and Insert Stability. *Viruses* **2020**, *12*, 61. [[CrossRef](#)] [[PubMed](#)]
30. Hall, M.P.; Unch, J.; Binkowski, B.F.; Valley, M.P.; Butler, B.L.; Wood, M.G.; Otto, P.; Zimmerman, K.; Vidugiris, G.; Machleidt, T.; et al. Engineered luciferase reporter from a deep sea shrimp utilizing a novel imidazopyrazinone substrate. *ACS Chem. Biol.* **2012**, *7*, 1848–1857. [[CrossRef](#)]
31. England, C.G.; Ehlerding, E.B.; Cai, W. NanoLuc: A Small Luciferase Is Brightening Up the Field of Bioluminescence. *Bioconjug. Chem.* **2016**, *27*, 1175–1187. [[CrossRef](#)]

32. Ryan, M.D.; King, A.M.; Thomas, G.P. Cleavage of foot-and-mouth disease virus polyprotein is mediated by residues located within a 19 amino acid sequence. *J. Gen. Virol.* **1991**, *72*, 2727–2732. [[CrossRef](#)]
33. Szymczak, A.L.; Vignali, D.A. Development of 2A peptide-based strategies in the design of multicistronic vectors. *Expert Opin. Biol. Ther.* **2005**, *5*, 627–638. [[CrossRef](#)]
34. Liu, Z.; Chen, O.; Wall, J.B.J.; Zheng, M.; Zhou, Y.; Wang, L.; Vaseghi, H.R.; Qian, L.; Liu, J. Systematic comparison of 2A peptides for cloning multi-genes in a polycistronic vector. *Sci. Rep.* **2017**, *7*, 2193. [[CrossRef](#)]
35. Szymczak, A.L.; Workman, C.J.; Wang, Y.; Vignali, K.M.; Dilioglou, S.; Vanin, E.F.; Vignali, D.A. Correction of multi-gene deficiency in vivo using a single ‘self-cleaving’ 2A peptide-based retroviral vector. *Nat. Biotechnol.* **2004**, *22*, 589–594. [[CrossRef](#)]
36. Donnelly, M.L.L.; Hughes, L.E.; Luke, G.; Mendoza, H.; Ten Dam, E.; Gani, D.; Ryan, M.D. The ‘cleavage’ activities of foot-and-mouth disease virus 2A site-directed mutants and naturally occurring ‘2A-like’ sequences. *J. Gen. Virol.* **2001**, *82*, 1027–1041. [[CrossRef](#)]
37. Lai, C.J.; Zhao, B.T.; Hori, H.; Bray, M. Infectious RNA transcribed from stably cloned full-length cDNA of dengue type 4 virus. *Proc. Natl. Acad. Sci. USA* **1991**, *88*, 5139–5143. [[CrossRef](#)]
38. Pu, S.Y.; Wu, R.H.; Yang, C.C.; Jao, T.M.; Tsai, M.H.; Wang, J.C.; Lin, H.M.; Chao, Y.S.; Yueh, A. Successful propagation of flavivirus infectious cDNAs by a novel method to reduce the cryptic bacterial promoter activity of virus genomes. *J. Virol.* **2011**, *85*, 2927–2941. [[CrossRef](#)]
39. Blaney, J.E., Jr.; Hanson, C.T.; Hanley, K.A.; Murphy, B.R.; Whitehead, S.S. Vaccine candidates derived from a novel infectious cDNA clone of an American genotype dengue virus type 2. *BMC Infect. Dis.* **2004**, *4*, 39. [[CrossRef](#)]
40. Li, X.F.; Deng, Y.Q.; Yang, H.Q.; Zhao, H.; Jiang, T.; Yu, X.D.; Li, S.H.; Ye, Q.; Zhu, S.Y.; Wang, H.J.; et al. A chimeric dengue virus vaccine using Japanese encephalitis virus vaccine strain SA14-14-2 as backbone is immunogenic and protective against either parental virus in mice and nonhuman primates. *J. Virol.* **2013**, *87*, 13694–13705. [[CrossRef](#)]
41. Suzuki, R.; de Borja, L.; Duarte dos Santos, C.N.; Mason, P.W. Construction of an infectious cDNA clone for a Brazilian prototype strain of dengue virus type 1: Characterization of a temperature-sensitive mutation in NS1. *Virology* **2007**, *362*, 374–383. [[CrossRef](#)]
42. Deng, C.L.; Zhang, Q.Y.; Chen, D.D.; Liu, S.Q.; Qin, C.F.; Zhang, B.; Ye, H.Q. Recovery of the Zika virus through an in vitro ligation approach. *J. Gen. Virol.* **2017**, *98*, 1739–1743. [[CrossRef](#)]
43. Messer, W.B.; Yount, B.; Hacker, K.E.; Donaldson, E.F.; Huynh, J.P.; de Silva, A.M.; Baric, R.S. Development and characterization of a reverse genetic system for studying dengue virus serotype 3 strain variation and neutralization. *PLoS Negl. Trop. Dis.* **2012**, *6*, e1486. [[CrossRef](#)]
44. Xie, X.; Muruato, A.; Lokugamage, K.G.; Narayanan, K.; Zhang, X.; Zou, J.; Liu, J.; Schindewolf, C.; Bopp, N.E.; Aguilar, P.V.; et al. An Infectious cDNA Clone of SARS-CoV-2. *Cell Host Microbe* **2020**, *27*, 841–848.e3. [[CrossRef](#)]
45. Xie, X.; Lokugamage, K.G.; Zhang, X.; Vu, M.N.; Muruato, A.E.; Menachery, V.D.; Shi, P.Y. Engineering SARS-CoV-2 using a reverse genetic system. *Nat. Protoc.* **2021**, *16*, 1761–1784. [[CrossRef](#)]
46. Kawano, H.; Rostapshov, V.; Rosen, L.; Lai, C. Genetic determinants of dengue type 4 virus neurovirulence for mice. *J. Virol.* **1993**, *67*, 6567–6575. [[CrossRef](#)]
47. Zellweger, R.M.; Prestwood, T.R.; Shresta, S. Enhanced infection of liver sinusoidal endothelial cells in a mouse model of antibody-induced severe dengue disease. *Cell Host Microbe* **2010**, *7*, 128–139. [[CrossRef](#)]
48. Chiu, Y.C.; Wu, K.L.; Kuo, C.H.; Hu, T.H.; Chou, Y.P.; Chuah, S.K.; Kuo, C.M.; Kee, K.M.; Changchien, C.S.; Liu, J.W.; et al. Endoscopic findings and management of dengue patients with upper gastrointestinal bleeding. *Am. J. Trop. Med. Hyg.* **2005**, *73*, 441–444. [[CrossRef](#)]